2011 50th IEEE Conference on Decision and Control and
European Control Conference (CDC-ECC)
Orlando, FL, USA, December 12-15, 2011

Non-collocated Feedback Stabilization of a Non-Uniform Euler-Bernoulli Beam with In-Domain Actuation

J. Schröck, T. Meurer, A. Kugi

Abstract— **For the stabilization of a flexible beam actuated by piezoelectric patches a Lyapunov-based control strategy is presented in terms of a non-collocated dynamic output feedback control. Thereby, a distributed-parameter Luenberger observer is incorporated to provide an estimate of the variables required by the control law. Besides the proof of asymptotic stability of the closed-loop system, the derived control concept is validated by experimental results.**

I. INTRODUCTION

The stabilization problem of flexible beams is a widely studied problem in the areas of aerospace as well as robotics, e.g., flexible space structures and lightweight robots. Typically, the control design is based on a finite-dimensional approximation of the governing partial differential equations. However, this early lumping approach may lead to non-satisfying control performance or, even worse, unstable closed-loop behavior induced by the well-known control and observer spillover problem [1], which originates from the neglected system dynamics. This can be avoided by the late lumping approach, which directly exploits the distributed-parameter description of the system in the control design.

In the following, a PDE-based control design for the stabilization of an Euler-Bernoulli beam actuated by a finite number of spatially distributed piezoelectric patches with additional tip mass is considered, see Fig. 1. While most control strategies for beam stabilization utilize boundary control, see, e.g., [2], the actuation of the beam considered in this contribution represents an in-domain actuation resulting in a non-uniform beam configuration. For this beam structure, a Lyapunov-based control design is presented, which is based on the collocation property of the actuator input and a certain system output. Thereby, asymptotic stability of the closed-loop system can be proven by means of semigroup theory and LaSalle's invariance principle. However, due to the fact that the respective collocated output is not measurable a distributed-parameter Luenberger observer is designed to obtain an estimation of the required quantity by considering available deflection measurements from the tip of the beam. Similarly to the stability proof of the controller, asymptotic stability of the observer error system can be proven. In order to guarantee the asymptotic stability of the closed-loop composite system including the controller and the observer a separation principle for generators of asymptotically stable semigroups is applied. Finally, the derived control design is validated by means of experimental results, which confirm the applicability of the presented approach.

The paper is organized as follows. In Sec. II, the abstract operator theoretic formulation of the equations of motion of the considered non-uniform Euler-Bernoulli beam is introduced. Based on this, the design of the non-collocated feedback control with observer is derived in Sec. III and validated by measurements results at a laboratory test bench in Sec. IV. Some final remarks conclude the paper.

II. MODELING AND ANALYSIS

In this contribution, the feedback stabilization problem is considered for a cantilevered Euler-Bernoulli beam with tip mass. The beam is actuated by pairs of piezo-electric patch actuators, where the patches on the front side (fs) and the patches on the back side (bs) are bonded symmetrically onto the beam structure, see Fig. 1. Utilizing an asymmetric

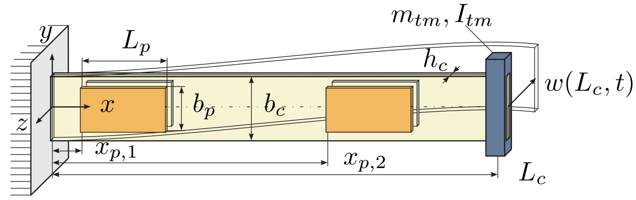

Fig. 1. Cantilever beam with pairs of patches.

voltage supply[1] $u_k^{fs(bs)}(t) = u_0 \overset{+}{(-)} u_k(t)$, $k = 1, \ldots, N_p$, this type of actuation allows to locally induce bending strains within the patch covered intervals $[x_{p,k}, x_{p,k} + L_p]$ of the beam domain defined by

$$\Lambda_k^\epsilon(x) = \left(\varrho^\epsilon(x - x_{p,k}) - \varrho^\epsilon(x - x_{p,k} - L_p)\right), \qquad (1)$$

where $\varrho^\epsilon(x) \in C^4(0, L_c)$ represents a smooth transition function from $\varrho^\epsilon(x) = 0$ for $x < -\epsilon/2$ to $\varrho^\epsilon(x) = 1$ for $x > \epsilon/2$. Here, L_c and L_p denote the length of the beam and the patches, respectively. Considering the individual patch contributions to stiffness, damping, and inertia, this configuration results in a beam model with spatially varying parameters such that the governing equations of motion for the beam deflection $w(x,t)$ are given by

$$\mu \partial_t^2 w + \gamma^e \partial_t w + \partial_x^2\big(EI \partial_x^2 w\big) = -\sum_{k=1}^{N_p} \Gamma_k u_k \qquad (2)$$

J. Schröck, T. Meurer, and A. Kugi are with the Automation and Control Institute (ACIN), Vienna University of Technology, Gusshausstrasse 27–29 / E376, 1040 Vienna, Austria {schroeck,meurer,kugi}@acin.tuwien.ac.at

[1]Here, $u_0 = 500$ V allows to balance the available supply voltage range $u_k^{fs(bs)}(t) \in [-500, +1500]$ V of the MFCs to $u_k(t) \in [-1000, +1000]$ V.

with the boundary conditions

$$
\begin{aligned}
&w = 0,\ \partial_x w = 0 && \text{for } x = 0,\\
&\left.\begin{aligned} &EI\partial_x^2 w + I_{tm}\partial_t^2\partial_x w = 0\\ &\partial_x\big(EI\partial_x^2 w\big) - m_{tm}\partial_t^2 w = 0\end{aligned}\right\} && \text{for } x = L_c.
\end{aligned} \tag{3}
$$

The parameter $\mu(x) = \mu_c + 2\sum_{k=1}^{N_p}\Lambda_k^\epsilon(x)\mu_p$ denotes the cross section density, $\gamma^e(x) = \gamma_c^e + 2\sum_{k=1}^{N_p}\Lambda_k^\epsilon(x)\gamma_p^e$ represents the viscous damping, $EI(x) = EI_c + 2\sum_{k=1}^{N_p}\Lambda_k^\epsilon(x)EI_p$ is the stiffness, and $\Gamma_k(x) = \Gamma_{p,k}\partial_x^2\Lambda_k^\epsilon(x)$ represents the in-domain actuation, where $\Gamma_{p,k}$ summarizes patch actuator specific parameters. Additionally, m_{tm} denotes the mass and I_{tm} the inertia of the tip mass. Here, the indices c, p and tm indicate the contributions of the carrier layer, the patches and the tip mass, respectively. The equations of motion (2), (3) can be directly determined by means of Hamilton's principle as shown in [3] for a cantilever without tip mass.

A. Abstract representation

For the following analysis, it is convenient to reformulate the governing equations as an abstract system in an appropriate Hilbert space. Consider the state vector $\boldsymbol{w} = [w_1(x,t), w_2(x,t), w_3(t), w_4(t)]^T$ with $w_1(x,t) = w(x,t)$, $w_2(x,t) = \partial_t w(x,t)$, $w_3(t) = w_2(x,t)|_{x=L_c}$, and $w_4(t) = (\partial_x w_2(x,t))_{x=L_c}$ together with the space $\mathcal{X} = H_C^2(0,L_c)\times L^2(0,L_c)\times\mathbb{R}\times\mathbb{R}$, where $H_C^2(0,L_c) = \{w_1 \in H^2(0,L_c)|\ w_1|_{x=0} = (\partial_x w_1)_{x=0} = 0\}$. The space $\mathcal{X}$ is a Hilbert space with the inner product

$$
\begin{aligned}
\langle \boldsymbol{w}^1, \boldsymbol{w}^2\rangle_{\mathcal{X}} = &\int_0^{L_c}\left(\mu w_2^1\overline{w_2^2} + EI\partial_x^2 w_1^1\overline{\partial_x^2 w_1^2}\right)\mathrm{d}x\\
&+ m_{tm}w_3^1\overline{w_3^2} + I_{tm}w_4^1\overline{w_4^2}
\end{aligned} \tag{4}
$$

for all $\boldsymbol{w}^1$, $\boldsymbol{w}^2 \in \mathcal{X}$ and the induced norm $\|\boldsymbol{w}\|_{\mathcal{X}} = \langle \boldsymbol{w},\boldsymbol{w}\rangle_{\mathcal{X}}^{1/2}$. Based on these preparations the model of the beam structure (2), (3) can be rewritten as

$$
\begin{aligned}
&\partial_t \boldsymbol{w} = A\boldsymbol{w} + \sum_{k=1}^{N_p}\boldsymbol{b}_k u_k, \quad t > 0\\
&\boldsymbol{w}(0) = \boldsymbol{w}_0 \in D(A).
\end{aligned} \tag{5}
$$

with the linear operator $A : D(A) \to \mathcal{X}$, $D(A) = \big(H^4(0,L_c)\cap H_C^2(0,L_c)\big)\times H_C^2(0,L_c)\times\mathbb{R}\times\mathbb{R}$, dense in $\mathcal{X}$ and the bounded input operators $\boldsymbol{b}_k \in \mathcal{L}(\mathbb{R},\mathcal{X})$, $k = 1,\ldots,N_p$ according to

$$
\begin{aligned}
A\boldsymbol{w} &= \begin{bmatrix} w_2\\ -\frac{1}{\mu}\left(\gamma^e w_2 + \partial_x^2\left(EI\partial_x^2 w_1\right)\right)\\ \frac{1}{m_{tm}}\left(\partial_x\left(EI\partial_x^2 w_1\right)\right)_{x=L_c}\\ -\frac{1}{I_{tm}}\left(EI\partial_x^2 w_1\right)_{x=L_c}\end{bmatrix}\\
\boldsymbol{b}_k &= \begin{bmatrix} 0 & -\frac{\Gamma_k}{\mu} & 0 & 0\end{bmatrix}^T.
\end{aligned} \tag{6}
$$

With this, the existence and uniqueness of the solution of (5) can be directly established.

B. Well-posedness of the model

By application of the Lumer-Phillips theorem, see, e.g., [2], it can be shown that the operator A is the infinitesimal generator of a C_0-semigroup of contractions. For this it has to be shown that the operator A is dissipative and there is a $\lambda_0 > 0$ such that the range of $(\lambda_0\mathcal{I} - A)$ is $\mathcal{X}$ with the identity operator $\mathcal{I}$.

Proposition 1. The operator A is dissipative.

Proof: Recognizing that $E(t) = \frac{1}{2}\langle \boldsymbol{w},\boldsymbol{w}\rangle_{\mathcal{X}}$ represents the total energy of the free system (5) a direct calculation shows that

$$
\frac{\mathrm{d}}{\mathrm{d}t}E = \langle A\boldsymbol{w},\boldsymbol{w}\rangle_{\mathcal{X}} = -\int_0^{L_c}\gamma^e(w_2)^2\mathrm{d}x \le 0,
$$

which implies the dissipativity of A.

Instead of verifying that $(\lambda_0\mathcal{I} - A) : \mathcal{X}\to\mathcal{X}$ is onto for $\lambda_0 > 0$ it is sufficient to show that the inverse operator A^{-1} exists and is bounded [4, Thm. 1.2.4].

Proposition 2. The operator A^{-1} exists and is bounded.

Proof: To show the existence of A^{-1} the equation $A\boldsymbol{w} = \boldsymbol{\zeta}$ with $\boldsymbol{w} \in D(A)$ is solved for a given $\boldsymbol{\zeta} \in \mathcal{X}$. Here, the solution can be directly determined as

$$
\begin{aligned}
w_1 = &\int_0^x\int_0^{p_3}\frac{1}{EI(p_2)}\int_{p_2}^{L_c}\int_{p_1}^{L_c}h_1(p_0)\mathrm{d}p_0\mathrm{d}p_1\mathrm{d}p_2\mathrm{d}p_3\\
&-\int_0^x\int_0^{p_3}\frac{1}{EI(p_2)}\left(h_2(L_c - p_2) + h_3\right)\mathrm{d}p_2\mathrm{d}p_3\\
w_2 = &\ \zeta_1\\
w_3 = &\ (\zeta_1)_{x=L_c}\\
w_4 = &\ (\partial_x\zeta_1)_{x=L_c},
\end{aligned} \tag{7}
$$

with the functions $h_1(x,t) = -\mu(x)\zeta_2(x,t) - \gamma^e(x)\zeta_1(x,t)$, $h_2(t) = m_{tm}\zeta_3(t)$, and $h_3(t) = I_{tm}\zeta_4(t)$. This proves the existence of A^{-1}. Given $\boldsymbol{\zeta} \in \mathcal{X}$, i.e. $\zeta_1 \in H_C^2(0,L_c)$, $\zeta_2 \in L^2(0,L_c)$ and $\zeta_3,\zeta_4 \in \mathbb{R}$ it follows that $\boldsymbol{w} \in ((H^4\cap H_C^2)\times H_C^2\times\mathbb{R}\times\mathbb{R}) = D(A)$. Furthermore, it can be shown that the boundedness of $\boldsymbol{\zeta}$ implies the boundedness of $\boldsymbol{w}$ such that $A^{-1} \in \mathcal{L}(\mathcal{X}, D(A))$.

Theorem 1. The operator A generates a C_0-semigroup of contractions $T(t)$.

Proof: The proof follows directly by application of the Lumer-Phillips theorem in view of Proposition 1 and 2.

Furthermore, it is assumed that $\boldsymbol{b}_k \in \mathcal{L}(\mathbb{R},\mathcal{X})$ is an admissible input operator such that with [5, Prop. 4.2.5 and Remark 4.1.3] the initial value problem (5) has a unique mild solution in $\mathcal{X}$ in the form

$$
\boldsymbol{w}(t) = T(t)\boldsymbol{w}_0 + \sum_{k=0}^{N_p}\int_0^t T(t-\tau)\boldsymbol{b}_k u(\tau)\mathrm{d}\tau \tag{8}
$$

for every $u(t) \in L_{loc}^2([0,\infty);\mathbb{R})$ and $\boldsymbol{w}_0 \in \mathcal{X}$.

III. FEEDBACK STABILIZATION

For stabilization of the piezo-actuated non-uniform Euler-Bernoulli beam a Lyapunov-based control strategy is proposed. Recalling that $E(t) = \frac{1}{2}\langle \boldsymbol{w}, \boldsymbol{w} \rangle_{\mathcal{X}}$, applying integration by parts and considering the boundary conditions (3) yields the change of energy along a solution trajectory of (5) in the form

$$\frac{\mathrm{d}}{\mathrm{d}t}E = -\int_0^{L_c} \left(\gamma^e (\partial_t w)^2 + \sum_{k=1}^{N_p} \Gamma_k \partial_t w u_k \right) \mathrm{d}x \leq -\sum_{k=1}^{N_p} u_k M_k, \tag{9}$$

with $M_k(t) = \int_0^{L_c} \Gamma_k \partial_t w(x,t) \mathrm{d}x$. From this, it directly follows that the control law

$$u_k = \kappa_k M_k \tag{10}$$

with $\kappa_k > 0$ renders $E(t)$ a Lyapunov functional candidate, which allows to prove the asymptotic stability of the closed-loop system.

A. Stability analysis

For the proof of asymptotic stability of (5) with (10) note that

$$u_k = \kappa_k M_k = \kappa_k \Gamma_{p,k} \int_0^{L_c} \partial_x^2 \Lambda_k^{\epsilon} \partial_t w \mathrm{d}x \tag{11}$$

such that the closed-loop system can be rewritten as

$$\begin{aligned} \partial_t \boldsymbol{w} &= \tilde{A}\boldsymbol{w}, \quad t > 0 \\ \boldsymbol{w}(0) &= \boldsymbol{w}_0 \in D(\tilde{A}) \end{aligned} \tag{12}$$

with the operator

$$\tilde{A}\boldsymbol{w} = \begin{bmatrix} w_2 \\ -\frac{1}{\mu}\left(\gamma^e w_2 + \partial_x^2 \left(EI\partial_x^2 w_1\right)\right) - \frac{1}{\mu}\sum_{k=1}^{N_p} \Gamma_k \kappa_k M_k \\ \frac{1}{m_{tm}}\left(\partial_x \left(EI\partial_x^2 w_1\right)\right)_{x=L_c} \\ -\frac{1}{I_{tm}}\left(EI\partial_x^2 w_1\right)_{x=L_c} \end{bmatrix} \tag{13}$$

defined on the domain $D(\tilde{A}) = D(A)$.

Theorem 2. The operator $\tilde{A}$ is the infinitesimal generator $\tilde{T}(t)$ of a C_0-semigroup of contractions. Moreover, $\tilde{T}(t)$ is asymptotically stable.

Proof: Utilizing the Lumer-Phillips Theorem the proof is similar to the procedure presented in Section II-B. For this note that the dissipativity of the operator is shown by (9) with $u_k(t) = \kappa_k M_k(t)$ and $\kappa_k > 0$. The proof of the existence of the inverse operator $(\tilde{A})^{-1}$ is identical to the proof of the existence of A^{-1} by solving the equation $\tilde{A}\boldsymbol{w} = \boldsymbol{\zeta}$. Thereby, the solution is equal to (7) with $h_1(x,t) = -\mu(x)\zeta_2(x,t) - \gamma^e(x)\zeta_1(x,t) - \sum_{k=1}^{N_p} \kappa_k \Gamma_k(x) M_k(t)$. As a result, by the Lumer-Phillips Theorem the operator $\tilde{A}$ is the infinitesimal generator of a C_0-semigroup of contractions.
In order to prove the asymptotic stability of the semigroup, LaSalle's invariance principle generalized for infinite-dimensional systems is applied [2, Thm. 3.64]. Considering the Lyapunov functional candidate $E(t)$, the invariance principle states that all solutions of the closed-loop system (12) asymptotically tend to the maximal invariant subset of the set $\mathcal{S} = \{\boldsymbol{w} \in \mathcal{X} | \frac{\mathrm{d}}{\mathrm{d}t}E(t) = 0\}$ provided that the solution trajectories are precompact in $\mathcal{X}$. This precompactness property can be verified by means of [2, Thm. 3.65]. For this, note that $(\tilde{A})^{-1}$ exists and is bounded. Since the embedding of $D(\tilde{A})$ into $\mathcal{X}$ is compact by the Sobolev embedding theorem [7] $(\tilde{A})^{-1}$ is also a compact operator in $\mathcal{X}$. In addition, by [6, Thm. A.3.46] the operator $\tilde{A}$ is closed. Hence, [8, Chap. 3, Thm. 6.29] implies that the resolvent $R(\lambda, \tilde{A}) = (\lambda\mathcal{I} - \tilde{A})^{-1}$ is compact for any λ in the resolvent set of $\tilde{A}$. Moreover, it can be easily seen from the definition of $\tilde{A}$ that $\mathbf{0}$ is in the range of $\tilde{A}$ such that the precompactness of the solution trajectories is ensured by [2, Thm. 3.65] and the invariance principle can be applied. Investigation of (9) directly yields $\mathcal{S} = \{\boldsymbol{w} \in \mathcal{X} | \frac{\mathrm{d}}{\mathrm{d}t}E(t) = 0\} = \{\boldsymbol{w} \in \mathcal{X} | \partial_t w(x,t) = w_2(x,t) = 0\}$. Hence, the maximal invariant set of $\mathcal{S}$ consists of the solutions $\boldsymbol{w}(x,t) \in \mathcal{X}$ satisfying the equations

$$\begin{aligned} 0 &= -\frac{1}{\mu}\partial_x^2\left(EI\partial_x^2 w_1\right) \\ 0 &= \frac{1}{m_{tm}}\left(\partial_x\left(EI\partial_x^2 w_1\right)\right)_{x=L_c} \\ 0 &= -\frac{1}{I_{tm}}\left(EI\partial_x^2 w_1\right)_{x=L_c}. \end{aligned} \tag{14}$$

Since the only possible solution in $\mathcal{S}$ is $\boldsymbol{w} = \mathbf{0}$ LaSalle's invariance principle implies that the solution of the closed-loop system (12) asymptotically approaches the origin as $t \to \infty$.

Note, the evaluation of the control law (11) requires the velocity profile of the beam deflection $\partial_t w(x,t)$. Since this information can be hardly obtained by measurements the derivation of an appropriate observer is presented in the following.

B. Observer design

Based on measurements at the tip of the beam the required velocity profile of the beam deflection is estimated by means of a distributed-parameter Luenberger observer. For this, the observer system with the state $\hat{w}(x,t)$ is chosen as a copy of the original system, i.e.

$$\mu\partial_t^2\hat{w} + \gamma^e\partial_t\hat{w} + \partial_x^2\left(EI\partial_x^2\hat{w}\right) = -\sum_{k=1}^{N_p}\Gamma_k u_k \tag{15}$$

with the boundary conditions adapted by the functions $l_1(t)$ and $l_2(t)$ in the form

$$\begin{aligned} &\hat{w} = 0,\ \partial_x\hat{w} = 0 && \text{for } x = 0, \\ &\left.\begin{aligned} &EI\partial_x^2\hat{w} + I_{tm}\partial_t^2\partial_x\hat{w} = l_1 \\ &\partial_x\left(EI\partial_x^2\hat{w}\right) - m_{tm}\partial_t^2\hat{w} = l_2 \end{aligned}\right\} && \text{for } x = L_c. \end{aligned} \tag{16}$$

Introduction of the estimation error $\breve{w}(x,t) = \hat{w}(x,t) - w(x,t)$ directly yields the observer error system, which is due to the linearity of the system equal to (15), (16) but with $\breve{w}(x,t)$ instead of $\hat{w}(x,t)$ and $u_k(t) = 0$. Similarly to the control design, the energy of the observer error system given by $\breve{E}(t) = \frac{1}{2}\langle \breve{\boldsymbol{w}}, \breve{\boldsymbol{w}} \rangle_{\mathcal{X}}$ represents a Lyapunov functional candidate since

$$\begin{aligned}\frac{\mathrm{d}}{\mathrm{d}t}\breve{E} = &-\int_0^{L_c} \gamma^e (\partial_t \breve{w})^2 \mathrm{d}x \\ &- l_2 \left(\partial_t \breve{w}\right)_{x=L_c} + l_1 \left(\partial_x \partial_t \breve{w}\right)_{x=L_c} \\ &\leq -l_2 \left(\partial_t \breve{w}\right)_{x=L_c} + l_1 \left(\partial_x \partial_t \breve{w}\right)_{x=L_c}\end{aligned} \quad (17)$$

with $l_1(t) = -\alpha_1 \left(\partial_x \partial_t \breve{w}(x,t)\right)_{x=L_c}$ and $l_2(t) = \alpha_2 \left(\partial_t \breve{w}(x,t)\right)_{x=L_c}$, $\alpha_1, \alpha_2 > 0$, is negative semi-definite.

Remark 1. Considering the boundary conditions (16) one recognizes that the functions $l_1(t)$ and $l_2(t)$ can be interpreted as a bending moment and a force acting at the position $x = L_c$. This clarifies that $(l_1(t), (\partial_x \partial_t \breve{w})_{x=L_c})$ and $(l_2(t), (\partial_t \breve{w})_{x=L_c})$ represent collocated power pairings, which allow to manipulate the energy stored in the observer error system.

The functions $l_1(t)$ and $l_2(t)$ are proportional to velocities only such that static deviations between the estimated and the measured signals are not considered. To improve the observer design, an extended Lyapunov functional, i.e.

$$V = \frac{1}{2}\langle \breve{\boldsymbol{w}}, \breve{\boldsymbol{w}} \rangle_{\mathcal{X}} + \frac{\alpha_3}{2}\left(\breve{w}|_{x=L_c}\right)^2 + \frac{\alpha_4}{2}\left((\partial_x \breve{w})_{x=L_c}\right)^2 \quad (18)$$

with $\alpha_3,\ \alpha_4 > 0$ is used. Hence, the change of $V(t)$ along a solution trajectory $\breve{w}(x,t)$ yields

$$\begin{aligned}\frac{\mathrm{d}}{\mathrm{d}t}V = &\frac{\mathrm{d}}{\mathrm{d}t}\breve{E} + \Big(\alpha_3 \breve{w}\partial_t \breve{w} + \alpha_4 \partial_x \breve{w} \partial_x \partial_t \breve{w}\Big)_{x=L_c} \\ &\leq \bigg(\partial_t \breve{w}\big(\alpha_3 \breve{w} - l_2\big) + \partial_x \partial_t \breve{w}\big(\alpha_4 \partial_x \breve{w} + l_1\big)\bigg)_{x=L_c}\end{aligned} \quad (19)$$

such that the choice

$$\begin{aligned}l_1 &= -\left(\alpha_1 \partial_x \partial_t \breve{w} + \alpha_4 \partial_x \breve{w}\right)_{x=L_c} \\ l_2 &= \left(\alpha_2 \partial_t \breve{w} + \alpha_3 \breve{w}\right)_{x=L_c}\end{aligned} \quad (20)$$

results in a dissipative observer error system. In order to prove the asymptotic stability of the observer error system note that (15), (16), (20) can be rewritten in the abstract form

$$\begin{aligned}\partial_t \breve{\boldsymbol{w}} &= \breve{A}\breve{\boldsymbol{w}}, \quad t > 0 \\ \breve{\boldsymbol{w}}(0) &= \breve{\boldsymbol{w}}_0 \in D(\breve{A})\end{aligned} \quad (21)$$

with $\breve{\boldsymbol{w}} = [\breve{w}_1(x,t), \breve{w}_2(x,t), \breve{w}_3(t), \breve{w}_4(t),] = [\breve{w}(x,t), \partial_t \breve{w}(x,t), (\partial_t \breve{w}(x,t))_{x=L_c}, (\partial_x \partial_t \breve{w}(x,t))_{x=L_c}]$ and the operator

$$\breve{A}\breve{\boldsymbol{w}} = \begin{bmatrix} \breve{w}_2 \\ -\frac{1}{\mu}\left(\gamma^e \breve{w}_2 + \partial_x^2\left(EI\partial_x^2 \breve{w}_1\right)\right) \\ \frac{1}{m_{tm}}\left(\partial_x\left(EI\partial_x^2 \breve{w}_1\right)\right)_{x=L_c} - \frac{1}{m_{tm}} l_2 \\ -\frac{1}{I_{tm}}\left(EI\partial_x^2 \breve{w}_1\right)_{x=L_c} + \frac{1}{I_{tm}} l_1 \end{bmatrix} \quad (22)$$

defined on the domain $D(\breve{A}) = (H^4 \cap H_C^2) \times H_C^2 \times \mathbb{R} \times \mathbb{R})$ dense in $\breve{\mathcal{X}}$. Here, $\breve{\mathcal{X}} = H_C^2(0, L_c) \times L^2(0, L_c) \times \mathbb{R} \times \mathbb{R}$ and the inner product is defined as

$$\begin{aligned}\langle \breve{\boldsymbol{w}}^1, \breve{\boldsymbol{w}}^2 \rangle_{\breve{\mathcal{X}}} = &\int_0^{L_c} \Big(\mu \breve{w}_2^1 \overline{\breve{w}_2^2} + EI\partial_x^2 \breve{w}_1^1 \overline{\partial_x^2 \breve{w}_1^2}\Big) \mathrm{d}x_1 \\ &+ m_{tm} \breve{w}_3^1 \overline{\breve{w}_3^2} + I_{tm} \breve{w}_4^1 \overline{\breve{w}_4^2} \\ &+ \alpha_3 \Big(\breve{w}_1^1 \overline{\breve{w}_1^2}\Big)_{x=L_c} + \alpha_4 \Big(\partial_x \breve{w}_1^1 \overline{\partial_x \breve{w}_1^2}\Big)_{x=L_c}\end{aligned} \quad (23)$$

for all $\breve{\boldsymbol{w}}^1, \breve{\boldsymbol{w}}^2 \in \breve{\mathcal{X}}$.

Theorem 3. The operator $\breve{A}$ is the infinitesimal generator $\breve{T}(t)$ of a C_0-semigroup of contractions. Moreover, $\breve{T}(t)$ is asymptotically stable.

Proof: The proof is similar to the proof of Theorem 2 by taking into account the Lyapunov functional can be represented by $V(t) = \frac{1}{2}\langle \breve{\boldsymbol{w}}, \breve{\boldsymbol{w}} \rangle_{\breve{\mathcal{X}}}$.

As a result, an estimation of the spatial-temporal system state $\breve{\boldsymbol{w}}$ can be obtained solely from the measurements of $(\partial_t w(x,t))_{x=L_c}$, $(\partial_t \partial_x w(x,t))_{x=L_c}$, $w(x,t)|_{x=L_c}$, and $(\partial_x w(x,t))_{x=L_c}$.

C. Stability of the composite system

The composite system consisting of the controlled cantilever beam and the observer error system can be represented in the extended state $\boldsymbol{w}^{ext} = [(\boldsymbol{w})^T, (\breve{\boldsymbol{w}})^T]^T \in \mathcal{X} \times \breve{\mathcal{X}}$ by

$$\begin{aligned}\partial_t \boldsymbol{w}^{ext} &= A^{ext}\boldsymbol{w}^{ext}, t > 0 \\ \boldsymbol{w}^{ext}(0) &= \boldsymbol{w}_0^{ext} \in D(A^{ext})\end{aligned} \quad (24)$$

with the operator

$$A^{ext}\boldsymbol{w}^{ext} = \begin{bmatrix} A & P \\ 0 & \breve{A} \end{bmatrix} \boldsymbol{w}^{ext} \quad (25)$$

defined on the domain $D(A^{ext}) = D(A) \times D(\breve{A})$. Here, P is a linear bounded operator, i.e. $P \in \mathcal{L}(\breve{\mathcal{X}}, \mathcal{X})$, given by

$$P\breve{\boldsymbol{w}} = \begin{bmatrix} 0 \\ -\frac{1}{\mu}\sum_{k=1}^{N_p} \Gamma_k \kappa_k \int_0^{L_c} \Gamma_k \partial_t \breve{w} \mathrm{d}x \\ 0 \\ 0 \end{bmatrix}. \quad (26)$$

Based on this, it can be verified by [9, Thm. 3] that the asymptotic stability of both the controlled system and the observer error system implies the asymptotic stability of the composite closed-loop system.

In the following, it is shown by experimental results on a laboratory test bench that the presented approach yields a highly efficient control strategy for vibration control of the piezo-actuated cantilever beam with tip mass.

IV. EXPERIMENTAL RESULTS

The experimental validation is performed by considering a cantilevered beam actuated by macro-fiber composite (MFC) patch actuators, see Fig. 2. The beam consists of a fiber reinforced composite material with dimensions $L_c = 0.406\,\mathrm{m}$, $b_c = 0.045\,\mathrm{m}$, and $h_c = 0.75 \times 10^{-3}\,\mathrm{m}$ and an end mass of $m_{tm} = 0.0126\,\mathrm{kg}$. The rotational inertia I_{tm} of the end mass is supposed to be zero. Two pairs of MFC patches (type

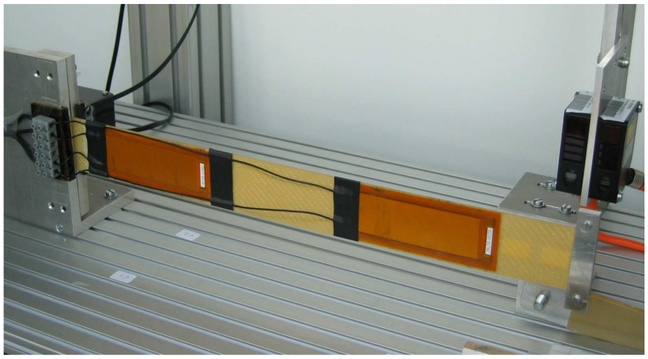

Fig. 2. Picture of the cantilevered beam with two pairs of MFC actuators and tip mass.

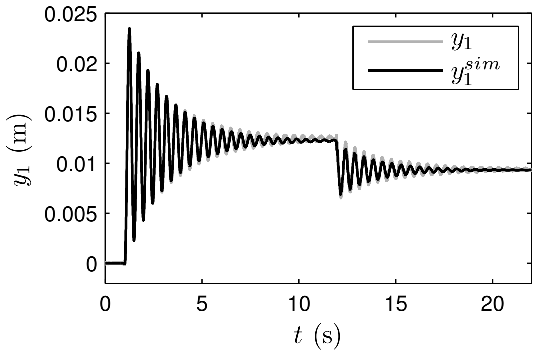

Fig. 3. Measured and simulated beam's tip deflection due to a voltage step of $u_1 = -500\,\mathrm{V}$ at the patch pair located at $x_{p,1}$ at $t = 1\,\mathrm{s}$ followed by a voltage step of $u_2 = 500\,\mathrm{V}$ at the patch pair at $x_{p,2}$ at $t = 12\,\mathrm{s}$.

$M8557P1$[1]) with an active area of dimension $L_p = 85 \times 10^{-3}\mathrm{m}$, $b_p = 57\times10^{-3}\mathrm{m}$, $h_p = 3\times10^{-4}\mathrm{m}$ are bonded to the beam at distances $x_{p,1} = 0.031\mathrm{m}$ and $x_{p,2} = 0.246\mathrm{m}$ from the clamped edge (cf. Fig. 1). For measurements two laser sensors located at $x_{m,1} = 0.88L_c$ m and $x_{m,2} = 0.95L_c$ m are used to obtain the deflection of the beam. With this and the assumption that the bending of the beam between $x = x_{m,1}$ and $x = L_c$ is negligible, the deflection and the angle at the beam's tip are approximated by extrapolation[2]. The measurements and the implementation of the control concept are realized using the real-time control board DS1103 of dSPACE, with a sampling time of $T_s = 0.2\,\mathrm{ms}$. The power supply is provided by two high-voltage four-quadrant power amplifiers PA05039 of Trek Inc.[1]

For the realization of the derived controller including the distributed-parameter observer a finite-dimensional approximation of (15), (16) is used by means of the Galerkin method. Here, the approach suggested in [3] is applied with the basis function chosen as the first 5 eigenmodes of a uniform cantilever beam.

Remark 2. For implementation purposes the control law (11) is evaluated by means of the spatial patch characteristics $\Lambda_k^0(x) = \lim_{\epsilon\to 0}\Lambda_k^\epsilon(x) = \sigma(x - x_{p,k}) - \sigma(x - x_{p,k} - L_p)$, where $\sigma(\cdot)$ denotes the Heaviside function. In this case, (11) includes the spatial derivative of the Dirac delta function $\delta(x)$ since $\partial_x^2\sigma(x) = \partial_x\delta(x)$ such that using integration by parts and assuming that $\left(\partial_x\Lambda_k^0(x)\right)_{x=L_c} = 0$ the control law evaluates to

$$\begin{aligned} u_k &= \kappa_k M_k \\ &= \kappa_k\Gamma_{p,k}\left[(\partial_t\partial_x w)_{x=x_{p,k}+L_{p,k}} - (\partial_t\partial_x w)_{x=x_{p,k}}\right] \end{aligned} \tag{27}$$

With this, the choice

$$u_k M_k = u_k\Gamma_{p,k}\left[(\partial_t\partial_x w)_{x=x_{p,k}+L_{p,k}} - (\partial_t\partial_x w)_{x=x_{p,k}}\right]$$

in view of (9), represents a power pairing including angular velocities and it follows by the collocation property that the effect of the voltages $u^k(t)$ can be interpreted as a pair of pointwise bending moments located at the boundary of the patches. In general, the functions $\Lambda_k^0(x)$ express discontinuous patch characteristics which require to consider the model of the cantilever beam (2), (3) in a weak or variational form. However, it can be shown that based on the weak formulation and the analysis of sesquilinear forms the feedback stability is preserved for discontinuous patch characteristics.

The parameters of the beam model are identified by minimizing the mean squares error between measured and simulated step responses based on the finite-dimensional approximation. At this point it should be emphasized that a hysteresis and creep compensation is utilized to cancel out the nonlinearities of the MFC patch actuators, for details see [10]. Note that the application of this compensator is crucial for the proposed modeling and design approach based on linear equations of motion of the MFC-actuated beam. As illustrated in Fig. 3, this procedure results in an excellent agreement between the measured and the simulated step responses $y_1 = w(x_{m,2}, t)$. The corresponding set of identified parameters is presented in detail in [10].

In view of the implementation of the observer, the velocity and the angular velocity used for stabilizing the observer error system, cf. (20), are determined from the measurements by means of appropriate filtering techniques. This allows to determine correct estimates for the quantities required in the control law (27) such that the beam structure can be efficiently stabilized in closed-loop. For illustrating the high control performance, experimental results concerning vibration suppression are presented. The beam is set into an oscillatory motion by a specified impulse generated by an impact hammer which is positioned at $x = 0.37$ m. In the uncontrolled case, this results in weakly damped vibrations due to the high flexibility of the beam, as shown in Fig. 4. Opposed to this, in the controlled case the oscillations are immediately damped out, see Fig. 5 (a), where Fig. 5 (b) depicts the voltage signals applied to the MFC patch pairs. These voltage signals result from the evaluation of (27) with estimates $(\partial_t\partial_x\check{w})_{x=x_{p,k}+L_{p,k}}$ and $(\partial_t\partial_x\check{w})_{x=x_{p,k}}$ obtained from the observer and subsequent processing by the

[1] Smart Material Corp., http://www.smart-material.com

[2] In this case the angle at the tip of the beam can be approximated by $\partial_x w(L_c, t) = \arctan[(w(x_{m,2}, t) - w(x_{m,1}, t)/(x_{m,2} - x_{m,1})]$.

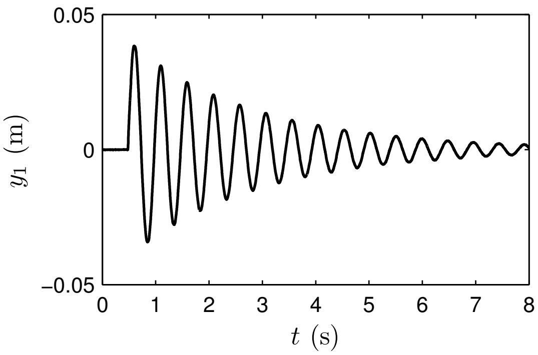

Fig. 4. Vibrations generated by an impact hammer positioned near the tip of the beam.

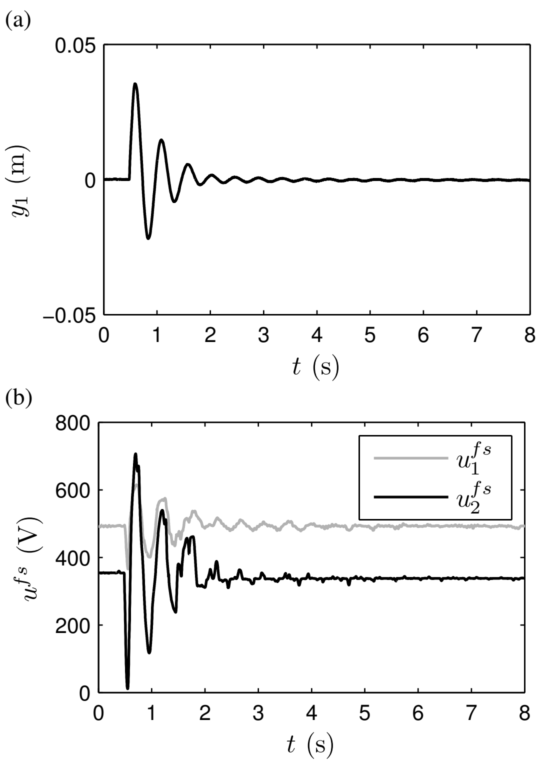

Fig. 5. Vibration control in case of an impact near the tip of the beam. (a) deflection $y_1(t) = w(x_{m,2}, t)$, (b) voltages applied to the MFC patch pairs, where u_0 of the patch pair located at $x_{p,1}$ is adapted to $u_0^{fs} = 500-150$ V and $u_0^{bs} = 500 + 150$ V in order to compensate an inherent deflection resulting from the manufacturing process of the beam.

hysteresis and creep compensator.

V. CONCLUSION AND FUTURE WORKS

In this contribution, a control concept in form of a non-collocated dynamic output feedback control for the stabilization of a cantilevered Euler-Bernoulli beam with in-domain actuation is presented. For this, based on the distributed-parameter description of the system a feedback controller with observer is derived by means of Lyapunov's theory including the proof of asymptotic stability of the closed-loop system using semigroup theory, LaSalle's invariance principle, and a separation principle for generators of asymptotically stable semigroups. In addition, the feedback control is validated by experimental results.

Future work is dedicated to the combination of the dynamic feedback controller with the feedforward control presented in [3], [10] within the so-called two-degrees-of-freedom control concept, see, e.g, [11], in order to realize robust trajectory tracking control for the flexible cantilever beam.

REFERENCES

[1] M. Balas, "Feedback Control of Flexible Systems," *Trans. Automat. Control*, vol. 23, no. 4, pp. 673–679, 1978.

[2] Z.-H. Luo, B.-Z. Guo, and Ö. Morgül, *Stability and Stabilization of Infinte Dimensional Systems with Applications*. London, Berlin, Heidelberg: Springer, 1999.

[3] J. Schröck, T. Meurer, and A. Kugi, "Flexible beam actuated by macro-fiber composite patches–Part I: Modelling and feedforward trajectory control," *SIAM Smart Material and Structures*, vol. 20, no. 1, 2011, 015015 (7 pages).

[4] Z. Liu and S. Zheng, *Semigroups Associated with Dissipative Systems*. Boca Raton, London: Chapman & Hall/CRC, 1999.

[5] M. Tucsnak and G. Weiss, *Observation and Control for Operator Semigroups*. Basel Boston Berlin: Birkhäuser, 2009.

[6] R. Curtain and H. Zwart, *An Introduction to Infinite–Dimensional Linear Systems Theory*. New York: Springer–Verlag, 1995.

[7] R. A. Adams and J. J. F. Fournier, *Sobolev Spaces*, 2nd ed. Amsterdam: Acadamic Press, 2003.

[8] T. Kato, *Perturbation Theory for Linear Operators*. Berlin: Springer, 1980.

[9] T. Meurer and A. Kugi, "Tracking control design for a wave equation with dynamic boundary conditions modeling a piezoelectric stack actuator," *Int. J. Robust. and Nonlinear Control*, vol. 21, no. 5, pp. 542–562, 2011.

[10] J. Schröck, T. Meurer, and A. Kugi, "Flexible beam actuated by macro-fiber composite patches–Part II: Hysteresis and creep compensation, experimental results," *SIAM Smart Material and Structures*, vol. 20, no. 1, 2011, 015016 (10 pages).

[11] T. Meurer, D. Thull, and A. Kugi, "Flatness–based tracking control of a piezoactuated Euler–Bernoulli beam with non–collocated output feedback: theory and experiments," *Int. J. Control*, vol. 81, no. 3, pp. 473–491, 2008.